

Inhibition of HPV18 E6/E7 Protein-Expressing HeLa Cell Proliferation Using Optimized De Novo CRISPR/Cas9 Constructs Delivered by the LL-37 Peptide

Niloofer Khairkhan¹ , Azam Bolhassani^{2,3*} , Reza Najafipour^{1,4*} , Ali Namvar³ , Alireza Milani² , Elnaz Agi³ , Ali Anvar³ , Mohammad Sadeq Khosravy⁵ 

¹Cellular and Molecular Research Center, Institute for Prevention of Non-Communicable Diseases, Qazvin University of Medical Sciences, Qazvin, Iran; ²Department of Hepatitis, AIDS and Blood-borne Diseases, Pasteur Institute of Iran, Tehran, Iran, Pasteur Institute of Iran, Tehran, Iran; ³Blood Diseases Research Center (BDRC), Iranian Comprehensive Hemophilia Care Center, Iran University of Medical Sciences (IUMS), Tehran, Iran; ⁴Genetics Research Center, University of Social Welfare and Rehabilitation Sciences, Tehran, Iran; ⁵WHO Collaborating Center for Reference and Research on Rabies, Pasteur Institute of Iran, Tehran, Iran

ARTICLE INFO

Original Article

Keywords: Cervical cancer, HPV18 E6/E7 oncoproteins, CRISPR-Cas9 gene editing, Cell-penetrating peptide, LL-37 peptide, Tumor suppression

Received: 18 Nov. 2024

Received in revised form: 3 Dec. 2024

Accepted: 25 Dec. 2024

DOI: 10.61186/JoMMID.12.4.278

*Correspondence

Email: azam.bolhassani@yahoo.com,

A_bolhasani@pasteur.ac.ir:

rnajafipour@gmail.com

Tel: +982166953311 Ext. 2240

Fax: +982166465132

© The Author(s)



ABSTRACT

Introduction: CRISPR/Cas-mediated gene editing has emerged as a transformative therapeutic modality for targeting oncogenic pathways in cancer. This technology enables precise disruption of oncogenic processes, such as tumor cell migration and invasion, and facilitates targeted tumor eradication. This study employed CRISPR/Cas9-mediated genome editing to disrupt the HPV18 E6 and E7 oncogenes, which are critical drivers of tumorigenesis in HPV-associated cancers. **Methods:** Optimized single-guide RNA (sgRNA) sequences were designed to target the HPV18 E6 and E7 oncogenes, along with the p105 promoter region, for CRISPR/Cas9-mediated genome editing. The sgRNA sequences were cloned into CRISPR/Cas9 expression vectors. HPV18-positive HeLa cells, were transfected *in vitro* with the recombinant vectors to assess gene editing efficiency. For the *in vivo* evaluation, C57BL/6 mice bearing HeLa-derived tumors received intravenous injections of LL-37 peptide-complexed recombinant vectors. The therapeutic efficacy of this approach was quantitatively compared to cisplatin treatment. **Results:** The dual E6/E7-targeted group exhibited a statistically significant reduction in tumor volume compared to all other groups, including the single E6-targeted group, the single E7-targeted group, the cisplatin-treated group, and the untreated control group ($P < 0.05$). LL-37 peptide demonstrated efficient delivery of CRISPR/Cas9 vectors into HeLa tumor cells, with an optimal nitrogen-to-phosphate (N/P) ratio of 5: 1, achieving high transfection efficiency without systemic toxicity. **Conclusion:** These findings establish CRISPR/Cas9-mediated gene editing as a potent therapeutic strategy for HPV-associated tumors and highlight LL-37 as a promising non-viral delivery platform for CRISPR/Cas9 constructs. This study is the first to demonstrate the *in vivo* efficacy of multiplexed sgRNA delivery targeting HPV18 oncogenes in a preclinical model.

INTRODUCTION

Human papillomavirus (HPV) infection, predominantly transmitted through sexual contact, is a significant etiological factor in various malignancies, including cervical, head and neck, and anogenital cancers [1]. Among the over 200 identified HPV types, high-risk variants, particularly genotypes 16 and 18, are classified as Group 1 carcinogens and are strongly implicated in oncogenesis. HPV16 and HPV18 account for over 70% of cervical cancer cases worldwide [2]. The oncogenic potential of HPVs is mediated by the E6 and E7 oncoproteins, which disrupt key tumor suppressor

pathways. Integration and expression of E6 and E7 drive malignancy by inactivating tumor suppressor proteins, including p53 and retinoblastoma (Rb) [3]. Prophylactic HPV vaccines (*e.g.*, Gardasil-9, Gardasil, and Cervarix) have significantly reduced the incidence of HPV-associated cancers but are ineffective against pre-existing infections [4]. Notably, HPV18 is more prevalent in squamous cell carcinoma (SCC) than in high-grade cervical intraepithelial neoplasia (CIN2/3) lesions. This suggests that the role of HPV18 in SCC progression may be underestimated, as CIN2/3 is often

used as an intermediate endpoint in cervical cancer research [5]. Cervical cancer patients with HPV18 infections exhibit poorer progression-free survival (PFS) and overall survival (OS) outcomes [6]. Given the global health burden of HPV18-associated malignancies, novel therapeutic strategies are urgently needed. The standard of care for HPV18-associated cervical cancer includes chemotherapy, radiation therapy, and surgical intervention. Specifically, cisplatin-based chemotherapy is commonly used for patients with metastatic or recurrent disease [7]. Targeting E6 and E7 oncoproteins using CRISPR/Cas9 represents a promising therapeutic strategy for HPV18-related cancers [8]. The CRISPR/Cas9 system uses a guide RNA (gRNA) to direct the Cas9 endonuclease to a specific genomic locus. Targeting relies on sequence complementarity between the gRNA and target DNA, along with a protospacer adjacent motif (PAM) sequence downstream of the target site. Upon successful target recognition, the Cas endonuclease induces a precise double-strand break (DSB) within the DNA [9]. Studies have demonstrated that CRISPR-Cas9-mediated knockout of the E6 and E7 oncogenes can effectively reduce tumor growth following a three-dose administration regimen [10-12]. Furthermore, CRISPR/Cas9 systems predominantly utilize the error-prone non-homologous end-joining (NHEJ) pathway for gene knockout [11]. Despite its considerable efficacy, the Cas9 nuclease exhibits the potential for off-target mutagenesis at unintended genomic loci. Currently, a suite of freely accessible computational tools, including CHOPCHOP (<https://chopchop.cbu.uib.no/>) [13], Cas-OFFinder (<http://www.rgenome.net/cas-offinder/>) [14], E-Crisp (<http://www.e-crisp.org/E-CRISP/>) [15], and CRISPOR (<http://crispor.tefor.net/>) [16], are invaluable for the rational design of guide RNAs that maximize on-target activity while minimizing the risk of off-target effects [17]. Conversely, efficient systemic delivery of CRISPR/Cas9 vectors remains a significant hurdle. Among the diverse non-viral delivery systems, cell-penetrating peptides (CPPs) have emerged as promising candidates due to their capacity for effective vaccine and therapeutic agent delivery, coupled with a favorable safety profile [18]. A prominent example is the LL-37 peptide, a cationic antimicrobial peptide that has demonstrated the ability to facilitate the cellular uptake of exogenous DNA *in vitro* and modulate immune responses *in vivo* [19-21]. Furthermore, studies have indicated that LL-37 peptides can stimulate the proliferation of B lymphocytes, natural killer (NK) cells, and dendritic cells, thereby promoting anti-tumor immunity and potentially facilitating tumor eradication [22, 23].

In our previous work, we successfully demonstrated the therapeutic potential of CRISPR/Cas9 for HPV16-associated tumors [24]. Building upon this foundation, the present study explored the therapeutic potential of CRISPR/Cas9 for HPV18-associated tumors.

Specifically, we developed a novel set of multi-guide RNAs (gRNAs) meticulously designed to target the E6 and E7 oncogenes. To enhance on-target specificity and minimize the potential for off-target effects, we leveraged established computational tools, including CRISPOR and CHOPCHOP, for the design of targeted gRNA sequences, which were then rigorously cross-validated using the Cas-OFFinder algorithm. Furthermore, to optimize systemic delivery of the CRISPR/Cas9 system for cancer therapy, we utilized the LL-37 peptide as an efficient cell-penetrating peptide carrier. In summary, our results demonstrate that the engineered CRISPR/Cas9 systems effectively curbed the activity of HPV18 E6 and E7, both *in vitro* and *in vivo*. Briefly, the significance of this article can be highlighted as follows: a) Pioneering the development and utilization of innovative multi-gRNAs designed to target both HPV18 E6 and E7 oncogenes; b) Utilizing LL-37 CPP to address the challenge of *in vivo* CRISPR/Cas9 delivery for HPV18-associated tumors; c) Employing a compact vector alongside CRISPR/Cas9 vector to improve transfection efficiency; d) Conducting a comparative analysis between the effectiveness of the CRISPR/Cas9 gene editing and a traditional chemotherapy agent (cisplatin).

MATERIAL AND METHODS

Bioinformatics study

Gene sequences. Reference gene sequences for the HPV-18 E6 (nucleotides 105–581), E7 (nucleotides 590–907), and p105 promoter (nucleotides 1–105) genes (GenBank accession number NC_001357.1) were retrieved from the National Center for Biotechnology Information (NCBI) database. These sequences served as the basis for subsequent bioinformatics analyses.

Selection of candidate target sites. The HPV18 E6, E7, and p105 gene sequences were inputted into the CHOPCHOP algorithm (<https://chopchop.cbu.uib.no/>) [13] to design candidate guide RNAs (gRNAs) approximately 20 nucleotides in length. The *Streptococcus pyogenes* CRISPR-Cas9 system requires a protospacer adjacent motif (PAM) with the consensus sequence NGG for target recognition [25]. CHOPCHOP employs a ranking system to evaluate gRNA candidates based on predicted on-target efficiency, genomic location, GC content, and potential off-target mismatches. The top three candidate gRNAs for each gene, as determined by CHOPCHOP, were selected for further evaluation. Subsequently, these candidate sequences were analyzed using the CRISPOR tool (<http://crispor.tefor.net/>) [16]. CRISPOR assigns a specificity score to each candidate site, with higher scores indicating a lower likelihood of off-target activity within the genome. It is important to note that the potential for off-target effects in human cell lines is by

influenced the genomic prevalence of compatible PAM sequences [26]. To predict potential off-target sites, CHOPCHOP utilizes the Bowtie algorithm [27], while CRISPOR employs BWA [28] for short-read alignment. In addition, the candidate gRNA sequences were cross-referenced using the Cas-OFFinder tool (<http://www.rgenome.net/cas-offinder/>) [14], which employs a distinct algorithm for identifying potential off-target binding sites. Following a comprehensive evaluation of the data generated by these bioinformatics tools, a single gRNA sequence for each target gene was selected for subsequent experiments.

***In vitro* study**

Construction of the CRISPR/Cas9 vectors. The PX330 (Addgene plasmid #42230) and PX458-GFP (Addgene plasmid #48138) plasmids were obtained from Addgene (Watertown, MA, USA). These vectors contain BbsI restriction enzyme sites to facilitate gRNA sequence insertion. Oligonucleotides encoding the selected gRNA sequences were synthesized by GenScript Biotech Corporation (Piscataway, NJ, USA) and subsequently cloned into the BbsI site of both the PX330 and PX458 vectors. The resulting plasmid constructs were verified by Sanger sequencing to confirm correct gRNA insertion.

Formation and characterization of the LL-37/vector complexes. Effective *in vivo* gene editing with CRISPR/Cas9 is contingent upon efficient delivery of the vector. Cell-penetrating peptides (CPPs) represent a compelling class of non-viral carriers for nucleic acid delivery due to their ability to facilitate cellular uptake and enhance cargo delivery with minimal associated toxicity [29]. In this study, the LL-37 cationic antimicrobial peptide (LLGDFFRKSKEKIGKEFKRIVQRIKDFLRNLPRTES-C-amide) was employed to investigate its efficacy in mediating CRISPR/Cas9 vector delivery both *in vitro* and *in vivo* [30, 31]. The detailed protocol for complex preparation was described in our previous publication [24]. Briefly, LL-37/vector complexes (nanoparticles) were formed at a nitrogen-to-phosphate (N/P) ratio of 5. The resulting complexes were characterized using a gel electrophoresis mobility shift assay to assess nucleic acid condensation, and their stability was evaluated in the presence of DNase I [32] and fetal bovine serum (FBS) [33]. The diameter and zeta potential (surface charge) of the LL-37/vector complexes were determined using scanning electron microscopy (SEM) (KYKY-EM3200 model, China) and a Zetasizer Nano ZS instrument (Malvern Panalytical, UK) at 25°C, respectively.

Transfection into HeLa cells. HeLa cells (HPV-18 positive, obtained from the National Cell Bank, Pasteur Institute of Iran) were maintained in Dulbecco's Modified Eagle's Medium (DMEM, Gibco) supplemented with 5% heat-inactivated fetal bovine

serum (FBS, Biosera) and 1% penicillin/streptomycin (Penstrep; Biosera) at 37°C in a humidified atmosphere containing 5% CO₂. Among HPV18-positive cell lines, HeLa cells, being derived from a cervical carcinoma, closely recapitulate the characteristics of cervical cancer cells, thus serving as a well-established and relevant model system for investigating host-virus interactions [34]. For transfection experiments, HeLa cells were seeded in 6-well plates at a density of 4×10^5 cells per well and incubated until reaching 80% confluency. Cells were then transfected with 1 µg of the PX458 CRISPR/Cas9 vector (encoding GFP as a reporter) either alone or co-transfected with an equimolar amount of a small empty pUC57 vector [35] using Lipofectamine 2000 (Invitrogen) according to the manufacturer's instructions. This co-transfection strategy with the empty vector was employed to maintain a consistent total amount of transfected DNA, controlling for potential vector size-dependent effects on transfection efficiency. To optimize transfection conditions, three different vector-to-Lipofectamine 2000 ratios (4 µg total vector with 4, 8, and 12 µl Lipofectamine 2000) were evaluated. In parallel experiments, the PX458 CRISPR/Cas9 vectors, with or without the empty pUC57 vector, were complexed with the LL-37 peptide for transfection. Transfection efficiency, as assessed by GFP expression, was analyzed using fluorescence microscopy (Invert Fluorescent Ceti, Korea) and flow cytometry (CyFlow SL, Partec, Germany) at an excitation wavelength of 488 nm, 48 hours post-transfection. Untransfected cells served as a negative control, while cells transfected with the pEGFP-N1 plasmid (Addgene plasmid #6085-1) using Lipofectamine 2000 served as a positive control for transfection efficiency.

T7 Endonuclease 1 (T7E1) assay. HeLa cells were seeded at a density of 4×10^5 cells per well and subsequently transfected with the recombinant PX458 CRISPR/Cas9 vectors using Lipofectamine 2000 (Thermo Fisher Scientific). Forty-eight hours post-transfection, genomic DNA flanking the targeted sites was extracted using the QIAwave DNA Extraction Kit (Qiagen, cat. no. 69556) according to the manufacturer's instructions. The target regions were then amplified by PCR using Phusion High-Fidelity DNA Polymerase and the primers listed in Table 1. Following amplification, purified PCR products (500 ng, QIAquick PCR Purification Kit, Qiagen, cat. no. 28104) were subjected to a denaturation and re-annealing step (95°C for 5 min, followed by slow cooling to room temperature) to allow for heteroduplex formation. These re-annealed products were subsequently digested with T7 Endonuclease I (20 U, New England Biolabs, cat. no. M0302L) at 37°C for 25 minutes. The resulting products were resolved by electrophoresis on a 1% agarose gel at 90 V for 1 hour. The T7E1 assay was not performed for the p105 promoter due to the short amplicon size (106 bp), which would preclude clear separation of cleaved and uncleaved fragments on an agarose gel. Band intensities

of cleaved and uncleaved DNA fragments were quantified using ImageJ software (NIH, USA). The gene modification rate was then calculated using the following

$$\text{formula [36]: \% Gene modification (GM)} = 100 \times (1 - (1 - \text{fraction cleaved})^{1/2})$$

Table 1. Oligonucleotide primers used for target amplification in the T7EI assay

Gene target	Primer type	Primer sequence (5'-3')
HPV18 E6	Forward	ATGGCGCGCTTTGAGGAT
	Reverse	GTGTCTCCATACACAGAGTCTG
HPV18 E7	Forward	GGTTGACCTTCTATGTCACG
	Reverse	CTGGCTTCACACTTACAACAC

Western blot analysis. To investigate the impact of CRISPR/Cas9-mediated gene editing on key cell cycle regulatory proteins, we assessed the expression levels of p53 and Rb. Given the established roles of HPV18 E6 and E7 in promoting the degradation and inactivation of p53 and Rb, respectively, and the potential influence of p105 gene editing, we focused on these targets. The optimized Western blot protocol employed in this study has been detailed in our previous publication [24], with modifications as described below. Briefly, forty-eight hours post-transfection, HeLa cells were harvested and lysed using RIPA buffer supplemented with protease and phosphatase inhibitors. Following protein quantification using Bradford assay, equal amounts of total protein (e.g., 20-30 µg) were resolved by sodium dodecyl-sulfate polyacrylamide gel electrophoresis (SDS-PAGE) on 12.5 % polyacrylamide gels. Proteins were then transferred to a nitrocellulose membrane. Membranes were blocked for 2 hours at room temperature with blocking buffer. Subsequently, membranes were incubated overnight at 4°C with primary antibodies against p53 (Cell Signaling Technology, cat. no. 9282S), Rb (BD Biosciences, cat. no. 610261), and β-actin (Cell Signaling Technology, cat. no. 4967) as a loading control. After washing extensively with TBST, membranes were incubated with a horseradish peroxidase (HRP)-conjugated secondary anti-mouse IgG antibody at room temperature for 4 hours. Protein bands were visualized by 3, 3'-diaminobenzidine (DAB, Sigma).

In vivo study. Given the potential for immunogenicity associated with the green fluorescent protein (GFP) marker present in the PX458 vector, subsequent *in vivo* experiments were conducted using the PX330 vector, which lacks this selection marker [37, 38]. For the treatment efficacy study, 6 × 10⁶ HeLa cells were subcutaneously inoculated into seven groups of five female C57BL/6 mice, aged 6-8 weeks. All CRISPR/Cas9 vectors were complexed with the LL-37 cell-penetrating peptide (CPP) at a nitrogen-to-phosphate (N/P) ratio of 5. Treatment groups (G1–G4) and control groups (G5–G7) received administrations according to the schedule outlined in Table 2. Tumor dimensions were measured using digital calipers, and tumor volume was calculated using the formula: V = 0.5 × (Length × Width²). To minimize observer bias, tumor measurements were performed by three independent, blinded observers. The health and well-being of the animals were monitored daily, with specific attention to appetite, grooming, activity levels, and coat condition. Each mouse was uniquely identified with an ear tag. Mice within the same treatment group were co-housed in polycarbonate cages under specific pathogen-free (SPF) conditions, maintained at a constant temperature of 22 ± 2°C and 50 ± 10% relative humidity, with a 12-hour light/dark cycle. The experimental endpoint for control groups was defined as the point at which tumors reached a pre-determined size or between days 42 and 50 post-inoculation, whichever occurred first. At the experimental endpoint, mice were humanely euthanized.

Table 2. *In vivo* treatment regimen

Group	Target	Injection route	Day 7 post-inoculation	Day 14 post-inoculation	Day 21 post-inoculation
G1	HPV18 E6	IV	HPV18 E6-targeting PX330 CRISPR/Cas9 / LL-37 Nanoparticles	HPV18 E6-targeting PX330 CRISPR/Cas9 / LL-37 Nanoparticles	HPV18 E6-targeting PX330 CRISPR/Cas9 / LL-37 Nanoparticles
G2	HPV18 E7	IV	HPV18 E7-targeting PX330 CRISPR/Cas9 / LL-37 Nanoparticles	HPV18 E7-targeting PX330 CRISPR/Cas9 / LL-37 Nanoparticles	HPV18 E7-targeting PX330 CRISPR/Cas9 / LL-37 Nanoparticles
G3	HPV18 E6 and HPV18 E7	IV	HPV18 E6-targeting PX330 CRISPR/Cas9 + HPV18 E7-targeting PX330 CRISPR/Cas9 / LL-37 Nanoparticles	HPV18 E6-targeting PX330 CRISPR/Cas9 + HPV18 E7-targeting PX330 CRISPR/Cas9 / LL-37 Nanoparticles	HPV18 E6-targeting PX330 CRISPR/Cas9 + HPV18 E7-targeting PX330 CRISPR/Cas9 / LL-37 Nanoparticles
G4	Chemotherapy Agent	IV	Cisplatin (5 mg/kg)	Cisplatin (5 mg/kg)	Cisplatin (5 mg/kg)
G5	Empty Vector Control	IV	PX330 CRISPR/Cas9 Empty Vector / LL-37 Nanoparticles	PX330 CRISPR/Cas9 Empty Vector / LL-37 Nanoparticles	PX330 CRISPR/Cas9 Empty Vector / LL-37 Nanoparticles
G6	Control	IV	PBS	PBS	PBS
G7	Peptide Control	IV	LL-37 Peptide	LL-37 Peptide	LL-37 Peptide

* **Abbreviations:** IV, intravenous; PBS, phosphate-buffered saline.

Statistical analysis. Differences in tumor volume between treatment and control groups were analyzed using a one-way analysis of variance (ANOVA) (GraphPad Prism, version 9.0, GraphPad Software, San Diego, California, USA). Prior to analysis, the assumptions of normality and homogeneity of variance were assessed. Data were presented as the mean \pm standard deviation (SD). Statistical significance was defined as $P < 0.05$.

Ethical considerations. This study received approval from the Biomedical Research Ethics Committee of Qazvin University of Medical Sciences (Approval ID: IR.QUMS.REC.1400.078).

In silico design and selection of gRNA candidates, and construction of the recombinant vectors. To optimize the specificity and efficacy of CRISPR/Cas9-mediated gene editing, a rigorous *in silico* selection of guide RNA (gRNA) candidates was performed. Target sequences within the HPV18 E6 and E7 oncogenes, as well as the p105 promoter region, were used as input for the bioinformatics tools CRISPOR, CHOPCHOP, and Cas-OFFinder to identify potential gRNA sequences with high on-target scores and minimal predicted off-target activity. Based on these analyses, a single gRNA sequence was selected for each target (Table 3). Subsequently, the selected gRNA sequences were successfully cloned into both PX330 and PX458 expression vectors. The correct insertion of the gRNA sequences into the respective vectors was confirmed by Sanger sequencing.

RESULTS

Table 3. Characteristics of CRISPR gRNA sequences targeting HPV18 E6, E7, and the p105 Promoter

Target	gRNA Sequence (5'–3')	PAM Sequence (5'–3')	Target Strand	CHOPCHOP Rank	GC Content (%)	CRISPOR CFD Score	Predicted Off-Targets
E6	AGCTTGTAGGGTCGCCGTGT	TGG	Negative	3	60	99	0
E7	ACGTTGTGGTTCGGCTCGTC	GGG	Negative	1	60	99	0
p105 Promoter	AAGGGAGTAACCGAAAACGGT	CGG	Positive	1	42	95	0

Abbreviations: CFD, cutting frequency determination; PAM, protospacer adjacent motif.

Characterization of LL-37 /vector nanoparticles. We investigated the interaction between the LL-37 cell-penetrating peptide (CPP) and PX330 or PX458 CRISPR/Cas9 vectors at varying nitrogen-to-phosphate (N/P) ratios. Our results indicated that stable peptide/DNA complexes were formed at an N/P ratio of 5, demonstrating protection against DNase I digestion and degradation in 10% serum *in vitro*. Scanning electron microscopy (SEM) revealed that the LL-37/vector nanoparticles (N/P ratio: 5) exhibited a size range of 110–140 nm, compared to the 40–80 nm size of the LL-37 peptide alone, consistent with previous reports [20, 24, 39, 40]. Zeta potential measurements indicated that the LL-37/vector nanoparticles possessed positive surface charges (+18.2 mV and +22.9 mV

for PX330 and PX458, respectively), in contrast to the negative surface charges of the naked vectors (-8.35 mV for PX330 and -6.58 mV for PX458). Notably, the physicochemical properties (size and zeta potential) of the vectors were not significantly affected by the relatively small size of the incorporated guide RNA (gRNA) sequences targeting E6, E7, and p105. Data for the LL-37/E7-PX458 nanoparticle complex are presented in Figure 1 as a representative example. Collectively, these findings indicate that LL-37 CPP effectively facilitates the formation of stable nanoparticles with the recombinant PX330 and PX458 CRISPR/Cas9 vectors, providing protection against enzymatic degradation in a serum-containing environment.

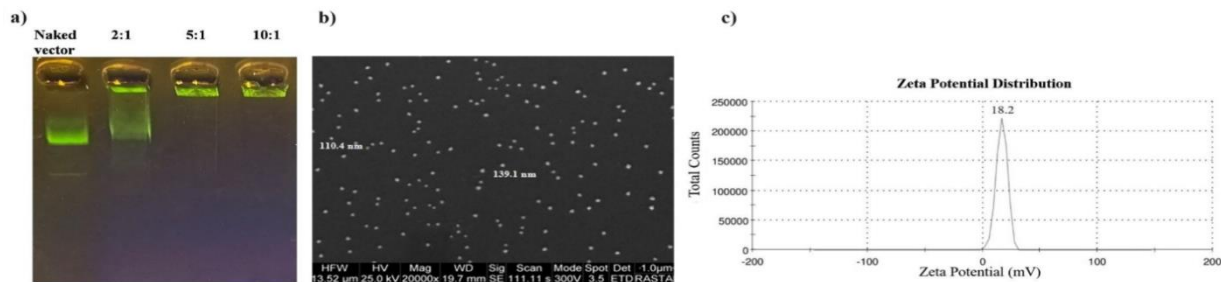


Fig. 1. Characterization of LL-37/E7-PX458 nanoparticle formation. (a) Gel retardation assay demonstrating the formation of LL-37/E7-PX458 nanoparticles at various nitrogen-to-phosphate (N/P) ratios. N/P ratios of 0, 2, 5, and 10 are indicated above the 1% agarose gel lanes. (b) Scanning electron microscopy (SEM) image of LL-37/E7-PX458 nanoparticles formed at an N/P ratio of 5. The image was acquired at a magnification of 20,000 \times . The diameter of the spherical LL-37/E7-PX458 nanoparticles was observed to be approximately 110–140 nm. (c) Dynamic light scattering (DLS) analysis illustrating the zeta potential distribution of LL-37/E7-PX458 nanoparticles. The nanoparticles exhibited a positive surface charge, with a zeta potential of +18.2 mV.

In vitro cell growth and transfection. HeLa cells harboring the HPV18 genome were transfected with either recombinant or empty PX458 CRISPR/Cas9 vectors, which incorporate a green fluorescent protein (GFP) marker. GFP expression was subsequently analyzed using fluorescence microscopy and flow cytometry to assess transfection efficiency. Transfection using Lipofectamine 2000 alone resulted in a low percentage of GFP-positive cells (E7-PX458: 10.67% \pm 0.83%; E6-PX458: 9.47% \pm 1.39%; PX458 empty vector: 9.23% \pm 2.59%). In contrast, co-transfection with pUC57 significantly enhanced transfection efficiency when using Lipofectamine 2000 (E7-PX458: 41.56% \pm 1.66%; E6-PX458: 38.99% \pm 2.53%; PX458 empty vector: 38.87% \pm 2.76%). This co-transfection method was significantly more efficient than transfection with PX458 vectors alone using Lipofectamine 2000 ($P < 0.05$). These results indicated that co-transfection of HeLa cells with both the recombinant or empty PX458 CRISPR/Cas9 vectors (2 μ g, approximately 9 kb) and a smaller pUC57 vector (2 μ g, approximately 3 kb) using Lipofectamine 2000 (4 μ L) significantly improved transfection efficiency. To evaluate the potential of LL-37 peptide to facilitate nanoparticle delivery, we repeated the experiment, introducing LL-37 peptide to assess the penetration of peptide/DNA nanoparticles into HeLa cells *in vitro*. The transfection efficiency using LL-37/PX458 nanoparticles alone was low (E7-PX458: 3.89% \pm 1.02%; E6-PX458: 4.47% \pm 1.61%; PX458 empty vector: 4.88% \pm 2.67%). However, the transfection efficiency of LL-37/(PX458 + pUC57) nanoparticles at an N/P ratio of 5:1 was significantly elevated compared to LL-37/PX458 alone (E7-PX458: 13.67% \pm 2.35%; E6-PX458: 12.45% \pm 2.05%; PX458 empty vector: 12.98% \pm 2.98%; $P < 0.05$). Consistent with the findings of Søndergaard *et al.* (2020), who employed a 1:1 ratio for transfecting large CRISPR/Cas9 vectors and small vectors into various cell lines, we utilized a similar 1:1 ratio for PX458 CRISPR/Cas9 vector and pUC57 vector in our transfections with Lipofectamine 2000 and LL-37 [35]. Our previous study also demonstrated a similar increase in transfection efficiency in TC1 and C3 cells (HPV16-positive cell lines) when a smaller vector was added to the transfection mixture, corroborating the findings of Søndergaard *et al.* (2020) [24]. Figure 2 illustrates the transfection efficiency of the recombinant E7-PX458

CRISPR/Cas9 vector, either alone or in combination with the empty pUC57 vector, using Lipofectamine 2000

T7E1 assay. To assess the on-target cleavage efficiency of the CRISPR/Cas9 system, PCR products amplified from genomic DNA of HeLa cells transfected with the recombinant PX458 vectors using Lipofectamine 2000 were subjected to the T7 Endonuclease I (T7EI) assay. As depicted in Figure 3, digestion of PCR amplicons from cells transfected with the recombinant PX458 CRISPR/Cas9 vectors with T7EI resulted in the appearance of cleaved DNA fragments, indicating successful gene editing. Specifically, for the E6 target, fragments of approximately 266 bp and 240 bp were observed, while digestion of the E7 amplicon yielded fragments of approximately 147 bp, 100 bp, and 50 bp. Conversely, PCR products from cells transfected with the empty PX458 vector remained undigested, displaying only a single, intact band of 266 bp for E6 and 147 bp for E7. These findings confirm the ability of the recombinant PX458 CRISPR/Cas9 vectors to efficiently induce double-strand breaks (DSBs) at the intended target sites within the HPV18 E6 and E7 oncogenes. Quantification of band intensities revealed gene modification rates exceeding 73% for both target sites (HPV18 E6 and E7), demonstrating effective induction of DSBs at the specific genomic locations.

Western blot analysis. To determine whether the HPV18 E6-, E7-, and p105-specific gRNA candidates could modulate the expression levels of key cell cycle regulatory proteins, Western blot analysis was performed to assess p53 and Rb protein abundance. In contrast to cells transfected with the empty PX458 CRISPR/Cas9 vector, our results demonstrated that targeting the HPV18 E6 and E7 genes effectively restored the expression levels of both p53 and Rb proteins (Figure 4). Comparison of band intensities on the Western blots indicated that targeting the E6 and E7 genes was more effective in stimulating the expression of these cell cycle regulatory proteins compared to targeting the p105 promoter. This observation suggests that the p105-specific gRNA was less efficient in modulating p53 and Rb expression under these experimental conditions, potentially due to the complexities of targeting a promoter region versus direct disruption of the oncogenes. Consequently, the p105-specific gRNA sequence was excluded from subsequent *in vivo* studies.

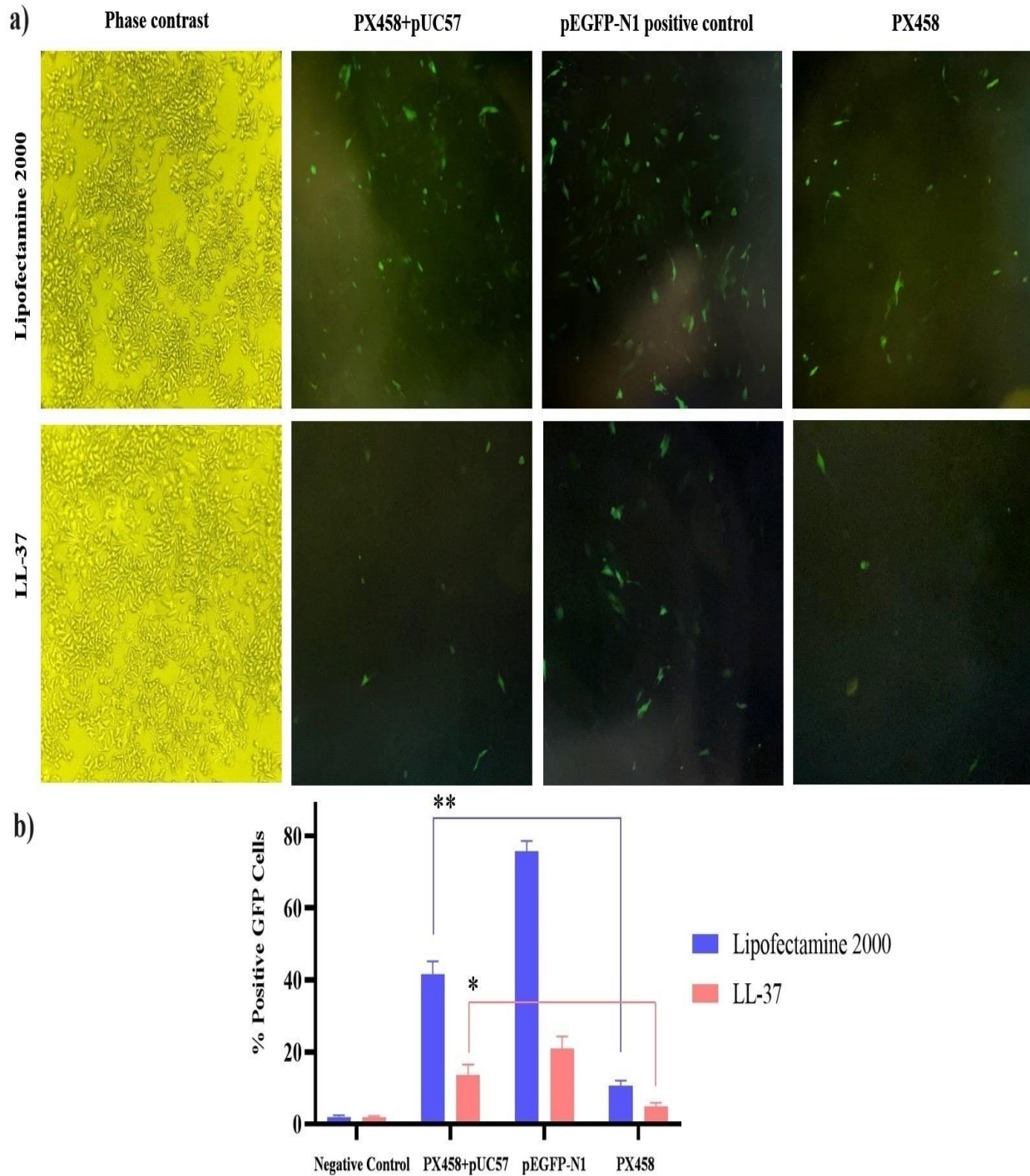


Fig. 2. Delivery of E7-PX458 CRISPR/Cas9 vector into HeLa cells using Lipofectamine 2000 and LL-37. (a) Representative microscopy images illustrating the delivery of the E7-PX458 CRISPR/Cas9 vector into HeLa cells 48 hours post-transfection using Lipofectamine 2000 (top panels) and LL-37 (bottom panels). Negative controls consisted of untransfected cells. Positive controls were transfected with pEGFP-N1 using Lipofectamine 2000 and LL-37. Cells were transfected with the E7-PX458 CRISPR/Cas9 vector, either alone or in combination with the pUC57 empty vector, using both Lipofectamine 2000 and LL-37; (b) Flow cytometry analysis of HeLa cells transfected with the E7-PX458 CRISPR/Cas9 vector using Lipofectamine 2000 and LL-37, with and without the pUC57 empty vector. The plots demonstrate a significant improvement in transfection efficiency upon co-transfection of the E7-PX458 CRISPR/Cas9 vector with the pUC57 vector for both Lipofectamine 2000-mediated (** $P < 0.01$) and LL-37-mediated (* $P < 0.05$) transfections.

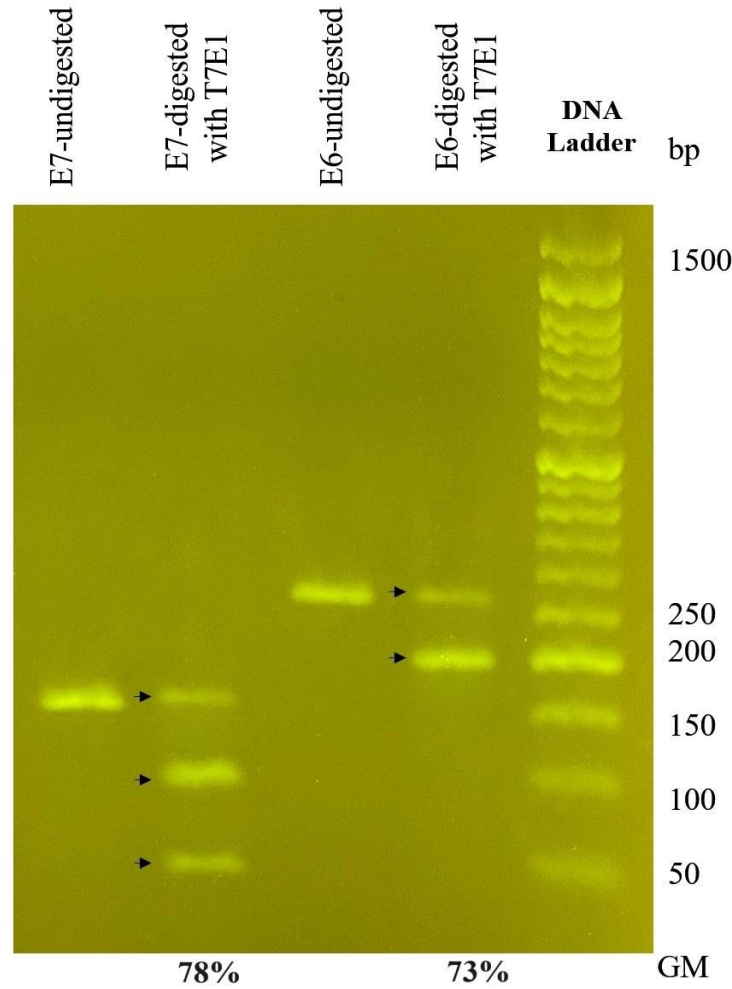


Fig. 3. T7EI assay on HeLa cells transfected with HPV18 E6- and E7-targeting CRISPR/Cas9 vectors. Genomic DNA was extracted from HeLa cells transfected with HPV18 E6- or E7-targeting PX458 CRISPR/Cas9 vectors, and the target regions were amplified by PCR. The resulting PCR products were subjected to T7EI digestion and resolved by agarose gel electrophoresis. The percentage of gene modification (% GM), as determined by T7EI analysis, is indicated below each lane. Black arrows indicate the positions of uncleaved (full-length) and cleaved DNA fragments.

In vivo study. To evaluate the therapeutic efficacy of E6 and E7 gene editing compared to chemotherapy (cisplatin) and control treatments, tumor growth was monitored in all groups for 42 days following subcutaneous inoculation of HPV18-positive HeLa cells. Upon reaching an average tumor volume of approximately 30 mm³, intravenous administration of the respective treatments or control solutions was initiated. Our findings demonstrated a significant reduction in tumor volume in the groups treated with recombinant CRISPR/Cas9 vectors (G1–G3) compared to all control groups (G5: PX330 empty vector, G6: PBS, and G7: LL-37; $P < 0.0001$) (Figure 5). Indeed, the rate of tumor growth in the treated groups was markedly slower than that observed in the control groups, particularly following the third dose of treatment administered on day 21 ($P < 0.0001$). Furthermore, the E7-treated (G2) and E6+E7-treated (G3) groups exhibited superior therapeutic outcomes compared to the E6-treated group alone. While

small tumor nodules (approximately 10 mm³) remained in the E7-treated group (G2) at the study endpoint, no detectable tumor was present in the E6+E7-treated group (G3) by day 35. Moreover, the difference in tumor volume between the cisplatin-treated group (G4) and the E6+E7-treated group (G3) was statistically significant ($P < 0.01$), whereas the difference between the cisplatin-treated group (G4) and the E7-treated group (G2) did not reach statistical significance. Targeting E6 alone (G1) appeared to be insufficient for effective treatment of HPV18-associated tumors; however, the cisplatin-treated group (G4) did not demonstrate significantly greater efficacy than the E6-treated group (G1; $P > 0.05$). The control groups (G5–G7) exhibited progressive tumor growth throughout the observation period (approximately days 14–42), although tumor volumes varied among these groups. No animals died or met the pre-defined criteria for early euthanasia during the study.

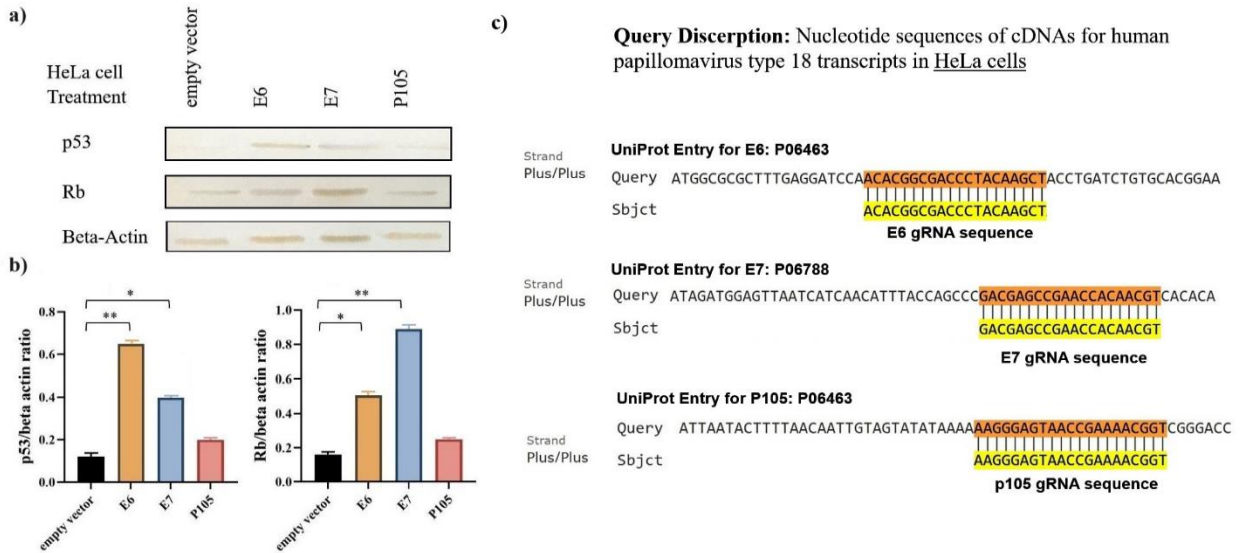


Fig. 4. Western blot analysis of cell cycle regulatory proteins following CRISPR/Cas9-mediated gene editing. (a) Representative Western blots showing the expression levels of Rb (130 kDa) and p53 (53 kDa) in HeLa cells transfected with target-specific (HPV18 E6 and E7) or control gRNA sequences. β -actin (45 kDa) was used as a loading control. Antibodies used were anti-Rb, anti-p53, and anti- β -actin. (b) Relative expression levels of p53 and Rb, normalized to β -actin, following transfection with target-specific or control gRNA sequences. Statistical significance is indicated as $P < 0.05$ and $P < 0.01$. (c) Sequence alignment of guide RNA (gRNA) sequences with their corresponding target sequences from the human UniProt database. The alignments are shown for the E6, E7, and p105 target regions of human papillomavirus type 18 (HPV-18). Highlighted regions indicate perfect complementarity between the gRNA and the target DNA sequence, crucial for efficient on-target binding and gene editing.

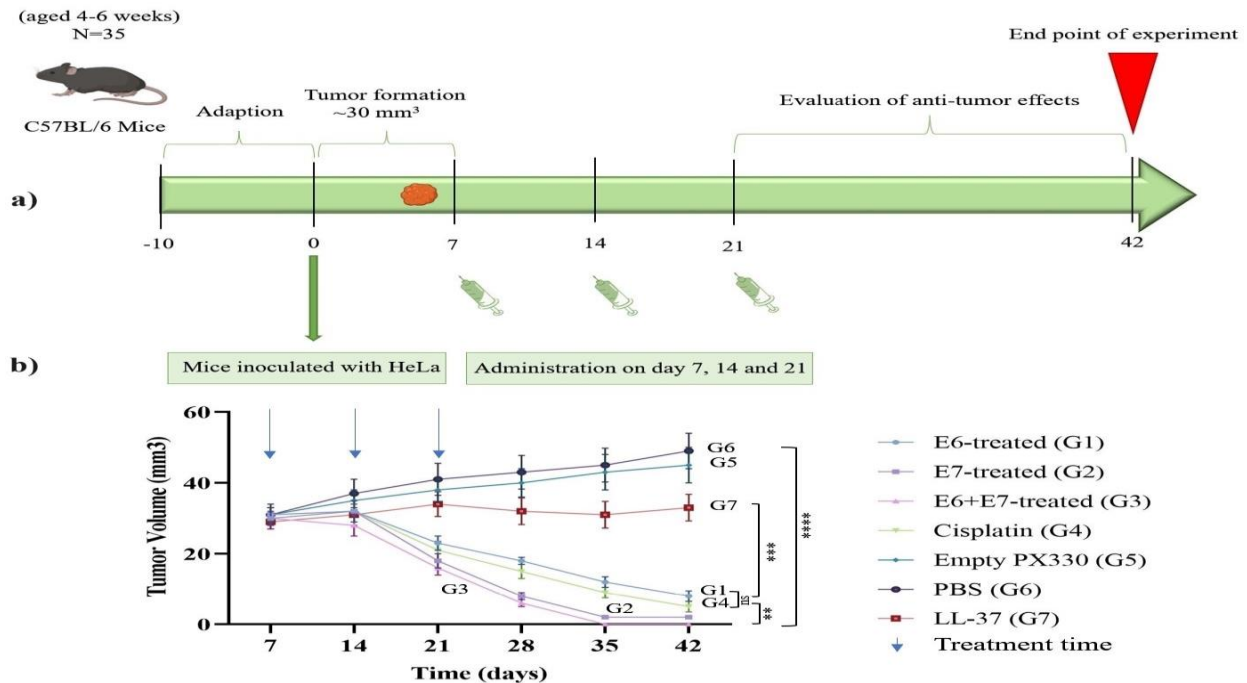


Fig. 5. *In vivo* tumor growth inhibition. (a) Schematic representation of the *in vivo* experimental design. (b) Tumor growth curves in C57BL/6 mice following subcutaneous implantation. Once tumors reached an average volume of 30 mm³, intravenous administrations of treatment or control agents were performed on days 7, 14, and 21 post-implantation (arrows indicate treatment days). Tumor volume was monitored for 42 days post-inoculation. Data are presented as mean \pm standard deviation (SD). Statistical significance is indicated as ns ($P > 0.05$, not significant), ** $P < 0.01$, *** $P < 0.001$, and **** $P < 0.0001$.

DISCUSSION

Among the diverse landscape of innovative cancer therapies, CRISPR/Cas9-mediated genome editing has

emerged as a transformative technology [41]. This approach holds significant therapeutic potential for HPV-associated malignancies. However, the successful

clinical translation of CRISPR/Cas9 hinges upon efficient and safe delivery, alongside the rigorous minimization of off-target effects [42]. To address these challenges, we developed a CRISPR/Cas9-based gene editing approach in C57BL/6 mice to inhibit HPV18-associated tumor growth. Furthermore, we employed the LL-37 cell-penetrating peptide to facilitate systemic delivery of the CRISPR/Cas9 system. In this study, optimal gRNA candidates were designed using computational prediction tools. A single, high-ranking candidate was chosen for each target—HPV18 E6, E7, and the p105 promoter—using CRISPOR, CHOPCHOP, and Cas-OFFinder, prioritizing those with a predicted off-target score of zero. To validate these computational predictions, subsequent *in vitro* and *in vivo* studies were conducted. The HPV18 E6-, E7-, and p105-specific gRNA candidates were cloned into PX330 and PX458 CRISPR/Cas9 vectors. Subsequently, the HPV18-positive HeLa cell line was transfected with the PX458 vectors using Lipofectamine 2000 and the LL-37 peptide. The capacity of the LL-37 peptide to facilitate the uptake of exogenous cargo has been previously demonstrated in several *in vitro* studies [43-45]. A significant hurdle in employing CRISPR/Cas9 systems is the inherent challenge of achieving efficient transfection, which can impede subsequent analyses. Søndergaard *et al.* (2020) proposed that the inclusion of small plasmids in the transfection mixture could enhance the efficiency of transfecting large CRISPR/Cas9 vectors into cancer cells [35]. To investigate this, Lipofectamine 2000 and LL-37 CPP were utilized with large recombinant or empty PX458 CRISPR/Cas9 vectors, with and without the addition of a small, empty pUC57 vector. Our findings corroborated their observation, demonstrating enhanced GFP expression in cells co-transfected with PX458 CRISPR/Cas9 vectors and the pUC57 vector. Thus, the efficiency of transfecting HeLa cancer cells with large vectors, whether using Lipofectamine 2000 or LL-37 CPP, can be improved by the inclusion of a smaller plasmid. This enhancement is likely attributable to the mechanism proposed by Søndergaard *et al.* (2020), whereby the transit of smaller plasmids through membrane pores may facilitate the subsequent entry of larger vectors by altering pore characteristics, thereby reducing the likelihood of entanglement [35]. Furthermore, the efficacy of gene editing was assessed using the T7EI assay. To assess this, we utilized the optimized co-transfection protocol involving pUC57 and CRISPR/Cas9 vectors delivered via Lipofectamine 2000, which yielded the highest transfection efficiency. These results validated the ability of the recombinant PX458 CRISPR/Cas9 vectors to efficiently induce double-strand breaks (DSBs) at the intended target sites within the HPV18 E6 and E7 oncogenes, with gene modification rates of at least 73%. The observed gene modification rates for HPV18 E6 and E7 may appear disproportionately high compared to the transfection efficiency. However, it is important to note that in

CRISPR/Cas9 knockout experiments, particularly those inducing apoptosis and reducing cell viability, transfection efficiency, as measured by GFP expression, can be underestimated. This is because cells undergoing apoptosis are unable to express the GFP marker from the transfected vector. Analysis of genomic DNA extracted from the entire cell population in the transfection mixture revealed gene modification rates that suggested a higher level of editing efficiency than that observed through fluorescence microscopy and flow cytometry. Alternatively, Western blot analysis demonstrated that efficiently targeting HPV18 E6 and E7 resulted in the downregulation of E6 and E7 protein levels, consequently upregulating pro-apoptotic cell cycle proteins. The E6- and E7-treated groups exhibited the most significant upregulation of p53 and Rb, respectively. These findings align with previous studies reported by Yoshida *et al.* (2019), Inturi *et al.* (2021), Noroozi *et al.* (2022), and Ehrke-Schulz *et al.* (2020) [46-49]. Yoshida *et al.* (2019) conducted an experiment on HeLa, HCS-2 and SKG-1 cell lines by CRISPR /Cas9 system, and reported that the p53 activity was reinstated by targeting and suppressing the E6 [46]. In an *in vitro* study, Inturi *et al.* (2021) showed that targeting HPV18 E6 or E7 genes in HeLa cells led to increased levels of p53/p21 and Rb/p21 [47]. Furthermore, Noroozi *et al.* (2022) reported that HPV18 E6 knockout resulted in an increase in p53 levels in HeLa cells [48]. Ehrke-Schulz *et al.* (2020) also demonstrated that HPV18-specific CRISPR/Cas9 E6 mutagenesis led to an increase in p53 protein levels [49]. The observation of increased Rb protein levels upon targeting HPV16 E6 with CRISPR/Cas9 knockout, and the increase in p53 protein levels upon targeting HPV16 E7 with CRISPR/Cas9 knockout, appears counterintuitive given the established understanding that targeting E6 typically leads to p53 upregulation, and targeting E7 typically leads to Rb upregulation. Several factors could account for this seemingly paradoxical observation. First, upon knockout of E6 or E7, cells may initiate compensatory mechanisms to counteract the loss of these viral oncoproteins. Second, given the extensive interplay of HPV oncoproteins with numerous cellular pathways, the knockout of E6 and E7 could indirectly influence other cellular proteins and pathways, potentially leading to the observed increase in Rb and p53. In this study, we demonstrated that targeting the coding regions of the viral oncogenes was more effective at inducing the expression of critical growth-regulating proteins compared to targeting the p105 promoter region. Consequently, the p105-targeting gRNA was excluded from further *in vivo* investigation. Despite advancements in CRISPR/Cas9 delivery technologies, significant challenges persist regarding biocompatibility, minimizing toxicity, and achieving tissue-specific targeting [50]. Fortunately, various novel biomaterials such as CPPs have been explored to overcome tissue barriers. CPPs have garnered considerable interest due to

their extended circulatory half-life, favorable biocompatibility and low toxicity profiles, enhanced tissue selectivity, and high transduction efficiency [18, 51]. In this context, CPP-based drug delivery systems have emerged as promising anticancer therapeutic agents with the potential for translation into clinical applications. In this study, we utilized the LL-37 peptide for systemic delivery of CRISPR/Cas9 vectors. The LL-37 peptide is an antimicrobial peptide recognized as a promising candidate for treating a broad spectrum of bacterial and viral infections. The net positive charge of LL-37 facilitates binding to the negatively charged bacterial membrane, potentially through the formation of toroidal pores [52]. Furthermore, electrostatic interactions can induce the formation of lipid domains in cancer cells [53]. Consequently, the overexpression of anionic membrane components such as sialylated gangliosides and phosphatidylserines heparin sulfate can enhance the cancer cell selectivity of cationic LL-37 [54]. However, it is important to note that the role of the LL-37 peptide in tumorigenesis appears to be context-dependent and may vary across different cancer types.

Studies have indicated that the LL-37 peptide can promote the growth and invasion of breast or ovarian cancer cells and upregulate neovascularization and angiogenesis [55, 56]. Additionally, the concentration of LL-37 CPP is a crucial determinant in balancing efficacy and potential cytotoxicity. Nevertheless, the precise mechanisms underlying the seemingly contradictory effects of LL-37 across various cancer types remain to be fully elucidated [54]. To evaluate the *in vivo* efficacy of our treatment strategy, HeLa cells were inoculated into C57BL/6 mice, which were subsequently treated with the recombinant CRISPR/Cas9 vectors. Our data demonstrated that the groups receiving treatment targeting E7 (G2) and E6+E7 (G3) achieved the most significant reduction in tumor volume compared to the control groups (G5: PX330 empty vector, G6: PBS, and G7: LL-37; $P < 0.0001$). Both E6 and E7 genes are critical oncogenes of HPV18. The E6 oncoprotein suppresses p53, and the E7 oncoprotein represses retinoblastoma protein (Rb) [57]. However, the E7 oncoprotein exhibits pleiotropic effects on cellular apoptosis, which are context-dependent and vary based on the specific virus and cell type, capable of either inducing or inhibiting p53-dependent or -independent apoptosis [58]. Conversely, studies have demonstrated that knockout of E6 enhances sensitivity to anticancer agents [46]. Therefore, for optimal therapeutic efficacy, the simultaneous targeting of both E6 and E7 oncogenes is recommended. While the difference in tumor volume between the E7-treated group (G2) and the E6+E7-treated group (G3) did not reach statistical significance at the study endpoint (day 42), our findings indicate that the E6+E7-treated group (G3) exhibited the most pronounced reduction in tumor burden. Moreover, the difference in tumor volume between the cisplatin-treated group (G4) and the E6+E7-treated group (G3) was

statistically significant ($P < 0.01$), whereas the difference in tumor volume between the cisplatin-treated group (G4) and the E7-treated group (G2) did not reach statistical significance. Our study demonstrated the successful reduction of tumor volume in mice through an effective delivery system, suggesting that the LL-37 antimicrobial peptide facilitated the effective systemic delivery of the CRISPR/Cas9 vectors. Furthermore, the absence of lethal off-target effects was observed, with a 100% survival rate across all treatment groups. Thus, careful consideration in the design of specific gRNA sequences is crucial for mitigating the potential for off-target effects associated with the CRISPR/Cas9 system. Data obtained from our *in vivo* study aligns with the findings of Jubair *et al.* (2019) [11] and Yoshiba *et al.* (2019) [46]. Jubair *et al.* (2019) investigated the therapeutic potential of an E7-targeting gRNA delivered via the PX330 CRISPR/Cas9 system in Rag1 mice bearing HeLa cell xenografts. Utilizing PEGylated lipoplexes for systemic plasmid delivery, they observed effective tumor growth suppression following three administrations (totaling 30 μg DNA) of the CRISPR/Cas9 HPV18-E7 construct [11]. Similarly, Yoshiba *et al.* (2019) explored the impact of HPV18-E6 targeting in a cervical cancer mouse model, employing a single intratumoral administration of a CRISPR/Cas9 plasmid delivered via adeno-associated virus (AAV). While they observed significant tumor growth suppression, they suggested that increasing the frequency of administration or utilizing multiple gRNAs could further enhance therapeutic efficacy [46]. Several studies have utilized C57BL/6 mice inoculated with HPV18-positive HeLa cells to investigate various aspects of tumor development and treatment. For instance, Arjomandnejad *et al.* (2014) inoculated C57BL/6 nude mice with HeLa cells and characterized the resulting cervical carcinoma model using immunohistochemistry (IHC) [59]. Furthermore, Galus *et al.* (2006) investigated the effect of Fluvastatin on heterotopic ossification induced by injecting HeLa cells into C57BL/6 mice [60]. To the best of our knowledge, Jubair *et al.* (2019) and Yoshiba *et al.* (2019) represent the only published studies utilizing CRISPR/Cas9 to target HPV-18 using a single guide RNA (gRNA). Our study is the first to employ multiple novel gRNA sequences targeting both the E6 and E7 oncogenes of HPV18, demonstrating promising results that compare favorably with the efficacy of cisplatin, a common chemotherapeutic agent. In conclusion, our findings demonstrate that employing the CRISPR/Cas9 system to target the key HPV18 oncoproteins, E6 and E7, represents a promising therapeutic strategy for HPV18-associated cancers, such as cervical carcinoma. Furthermore, this study explored the potential of the LL-37 peptide to facilitate *in vivo* CRISPR/Cas9 genome editing of HPV18, addressing a critical delivery challenge that, to the best of our knowledge, has not been previously investigated in the context of HPV18 CRISPR/Cas9 therapy. Our results

revealed that the group treated with the E6+E7 targeting construct (G3) exhibited a statistically significant reduction in tumor volume compared to the control groups (G5-G7) ($P < 0.0001$) and the group treated with cisplatin (G4) ($P < 0.01$). The key contributions of this study include: a) the pioneering development and application of novel multi-gRNA constructs specifically designed to target both the HPV18 E6 and E7 oncogenes; b) the innovative utilization of the LL-37 cell-penetrating peptide (CPP) to address the challenge of *in vivo* CRISPR/Cas9 delivery for HPV18-associated tumors; c) the strategic co-delivery of a compact vector alongside the CRISPR/Cas9 vector to enhance transfection efficiency; and d) a direct comparative evaluation of the efficacy of CRISPR/Cas9 gene editing against that of cisplatin, a standard chemotherapeutic agent. In summary, our data strongly suggest that CRISPR/Cas9-mediated genome editing offers a highly effective and specific approach, and that the utilization of LL-37/CRISPR/Cas9 nanoparticles holds significant potential as a robust delivery system to overcome the inherent challenges of *in vivo* nucleic acid delivery.

ACKNOWLEDGEMENT

This work was supported by the Elite Researcher Grant Committee under award number [Grant No. 4000080] from the National Institute for Medical Research Development (NIMAD), Tehran, Iran.

The individual contributions of the authors are as follows: N.K. and A.B. conceptualized the study and designed the experiments; N.K., A.B., R.N., and F.R. conducted the laboratory experiments and collected the data; A.N. and A.A. contributed to data acquisition and analysis; N.K., A.N., A.M., E.A., A.A., and M.S.K. were involved in project administration and management; N.K., A.B., and R.N. performed the data analysis and interpretation; N.K. drafted the initial manuscript; and N.K., A.B., R.N., F.R., A.N., A.M., E.A., A.A., and M.S.K. critically reviewed and edited the manuscript

CONFLICTS OF INTEREST

The authors declare that they have no conflicts of interest associated with this manuscript.

REFERENCES

1. Muñoz N, Castellsagué X, de González AB, Gissmann L. HPV in the etiology of human cancer. *Vaccine*. 2006; 24: S1-S10.
2. Bruni LAG, Serrano B, Mena M, Collado JJ, Gómez D, Muñoz J, Bosch FX, de Sanjosé S. ICO/IARC Information Centre on HPV and Cancer (HPV Information Centre). Human Papillomavirus and Related Diseases in the World. Summary Report 22 October 2021.
3. Santacroce L, Di Cosola M, Bottalico L, Topi S, Charitos IA, Ballini A, Inchingolo F, Cazzolla AP, Dipalma G. Focus on

HPV infection and the molecular mechanisms of oral carcinogenesis. *Viruses* 2021; 13: 559.

4. Peng S, Ferrall L, Gaillard S, Wang C, Chi WY, Huang CH, Roden RB, Wu TC, Chang YN, Hung CF. Development of DNA vaccine targeting E6 and E7 proteins of human papillomavirus 16 (HPV16) and HPV18 for immunotherapy in combination with recombinant vaccinia boost and PD-1 antibody. *M.Bio*. 2021;12: e03224-03220.
5. Bulk S, Berkhof J, Rozendaal L, Daalmeijer N, Gök M, De Schipper F, Van Kemenade F, Snijders P, Meijer C. The contribution of HPV18 to cervical cancer is underestimated using high-grade CIN as a measure of screening efficiency. *Br. J. Cancer* 2007; 96: 1234-1236.
6. Xu Y, Qiu Y, Yuan S, Wang H. Prognostic implication of human papillomavirus types in cervical cancer patients: a systematic review and meta-analysis. *Infect. Agents Cancer* 2020; 15: 1-9.
7. Khairkhah N, Bolhassani A, Najafipour R. Current and future direction in treatment of HPV-related cervical disease. *J. Mol. Med.* 2022; 100: 829-845.
8. Pal A, Kundu R. Human papillomavirus E6 and E7: the cervical cancer hallmarks and targets for therapy. *Front. Microbiol.* 2020; 10: 3116.
9. Ghaemi A, Bagheri E, Abnous K, Taghdisi SM, Ramezani M, Alibolandi M. CRISPR-cas9 genome editing delivery systems for targeted cancer therapy. *Life Sci.* 2021; 267: 118969.
10. Zhen S, Hua L, Takahashi Y, Narita S, Liu YH, Li Y. In vitro and in vivo growth suppression of human papillomavirus 16-positive cervical cancer cells by CRISPR/Cas9. *Biochem. Biophys. Res. Commun.* 2014; 450: 1422-1426.
11. Jubair L, Fallaha S, McMillan NA. Systemic delivery of CRISPR/Cas9 targeting HPV oncogenes is effective at eliminating established tumors. *Mol. Ther.* 2019; 27: 2091-2099.
12. Chen Y, Jiang H, Wang T, He D, Tian R, Cui Z, Tian X, Gao Q, Ma X, Yang, J. In vitro and in vivo growth inhibition of human cervical cancer cells via human papillomavirus E6/E7 mRNAs' cleavage by CRISPR/Cas13a system. *Antiviral Research* 2020; 178: 104794.
13. Labun K, Montague TG, Krause M, Torres Cleuren YN, Tjeldnes H, Valen E. CHOPCHOP v3: expanding the CRISPR web toolbox beyond genome editing. *Nucleic Acids Research* 2019; 47: W171-W174.
14. Bae S, Park J, Kim JS. Cas-OFFinder: a fast and versatile algorithm that searches for potential off-target sites of Cas9 RNA-guided endonucleases. *Bioinformatics* 2014; 30: 1473-1475.
15. Heigwer F, Kerr G, Boutros M. E-CRISP: fast CRISPR target site identification. *Nature Methods* 2014; 11: 122-123.

16. Concordet JP, Haeussler M. CRISPOR: intuitive guide selection for CRISPR/Cas9 genome editing experiments and screens. *Nucleic Acids Research* 2018; 46: W242-W245.
17. Rajan A, Shrivastava S, Kumar A, Singh AK, Arora PK. CRISPR-Cas system: from diagnostic tool to potential antiviral treatment. *Applied Microbiology and Biotechnology* 2022; 1-15.
18. Khairkhah N, Namvar A, Bolhassani A. Application of cell penetrating peptides as a promising drug carrier to combat viral infections. *Mol. Biotechnol.* 2023; 1-16.
19. Sandgren S, Wittrup A, Cheng F, Jönsson M, Eklund E, Busch S, Belting M. The human antimicrobial peptide LL-37 transfers extracellular DNA plasmid to the nuclear compartment of mammalian cells via lipid rafts and proteoglycan-dependent endocytosis. *Journal of Biological Chemistry* 2004; 279: 17951-17956.
20. Khairkhah N, Bolhassani A, Agi E, Namvar A, Nikyar A. Immunological investigation of a multiepitope peptide vaccine candidate based on main proteins of SARS-CoV-2 pathogen. *PLoS One* 2022; 17: e0268251.
21. Aloul KM, Nielsen JE, Defensor EB, Lin JS, Fortkort JA, Shamloo M, Cirillo JD, Gombart AF, Barron AE. Upregulating human cathelicidin antimicrobial peptide LL-37 expression may prevent severe COVID-19 inflammatory responses and reduce microthrombosis. *Frontiers in Immunology* 2022; 13: 880961.
22. Büchau AS, Morizane S, Trowbridge J, Schaubert J, Kotol P, Bui JD, Gallo RL. The host defense peptide cathelicidin is required for NK cell-mediated suppression of tumor growth. *The Journal of Immunology* 2010; 184: 369-378.
23. Yang B, Good D, Mosaib T, Liu W, Ni G, Kaur J, Liu X, Jessop C, Yang L, Fadhil R. Significance of LL-37 on immunomodulation and disease outcome. *BioMed. Research International* 2020; 2020: 8349712.
24. Khairkhah N, Bolhassani A, Rajaei F, Najafipour R. Systemic delivery of specific and efficient CRISPR/Cas9 system targeting HPV16 oncogenes using LL-37 antimicrobial peptide in C57BL/6 mice. *J. Med. Virol.* 2023; 95: e28934.
25. Xiang X, Li C, Chen X, Dou H, Li Y, Zhang X, Luo Y. CRISPR/Cas9-mediated gene tagging: a step-by-step protocol. In *CRISPR Gene Editing* (Springer) 2019; 255-269.
26. Fu Y, Foden JA, Khayter C, Maeder ML, Reyon D, Joung JK, Sander JD. High-frequency off-target mutagenesis induced by CRISPR-Cas nucleases in human cells. *Nature Biotechnology* 2013; 31: 822-826.
27. Langmead B, Trapnell C, Pop M, Salzberg SL. Ultrafast and memory-efficient alignment of short DNA sequences to the human genome. *Genome Biology* 2009; 10: 1-10.
28. Li H, Durbin R. Fast and accurate short read alignment with Burrows-Wheeler transform. *Bioinformatics* 2009; 25: 1754-1760.
29. Sadeghian I, Heidari R, Sadeghian S, Raei MJ, Negahdaripour M. Potential of cell-penetrating peptides (CPPs) in delivery of antiviral therapeutics and vaccines. *European Journal of Pharmaceutical Sciences* 2022; 169: 106094.
30. Tripathi S, Wang G, White M, Qi L, Taubenberger J, Hartshorn KL. Antiviral activity of the human cathelicidin, LL-37, and derived peptides on seasonal and pandemic influenza A viruses. *PLoS One* 2015; 10: e0124706.
31. Currie SM, Findlay EG, McHugh BJ, Mackellar A, Man T, Macmillan D, Wang H, Fitch PM, Schwarze J, Davidson DJ. The human cathelicidin LL-37 has antiviral activity against respiratory syncytial virus. *PLoS One* 2013; 8: e73659.
32. Moret I, Peris JE, Guillem VM, Benet M, Revert F, Dasí F, Crespo A, Aliño SF. Stability of PEI-DNA and DOTAP-DNA complexes: effect of alkaline pH, heparin and serum. *Journal of Controlled Release* 2001; 76: 169-181.
33. Sadeghian F, Hosseinkhani S, Alizadeh A, Hatefi A. Design, engineering and preparation of a multi-domain fusion vector for gene delivery. *International Journal of Pharmaceutics* 2012; 427: 393-399.
34. Masters JR. HeLa cells 50 years on: the good, the bad and the ugly. *Nat. Rev. Cancer* 2002; 2: 315-319.
35. Søndergaard JN, Geng K, Sommerauer C, Atanasoai I, Yin X, Kutter C. Successful delivery of large-size CRISPR/Cas9 vectors in hard-to-transfect human cells using small plasmids. *Commun. Biol.* 2020; 3: 319.
36. Guschin DY, Waite AJ, Katibah GE, Miller JC, Holmes MC, Rebar EJ. A rapid and general assay for monitoring endogenous gene modification. In *Engineered zinc finger proteins*, (Springer) 2010; 247-256.
37. Skelton D, Satake N, Kohn D. The enhanced green fluorescent protein (eGFP) is minimally immunogenic in C57BL/6 mice. *Gene Therapy* 2001; 8: 1813-1814.
38. Ansari AM, Ahmed AK, Matsangos AE, Lay F, Born LJ, Marti G, Harmon JW, Sun Z. Cellular GFP toxicity and immunogenicity: potential confounders in in vivo cell tracking experiments. *Stem Cell Reviews and Reports* 2016; 12: 553-559.
39. Comune M, Rai A, Cherreddy KK, Pinto S, Aday S, Ferreira AF, Zonari A, Blersch J, Cunha R, Rodrigues R. Antimicrobial peptide-gold nanoscale therapeutic formulation with high skin regenerative potential. *J. Controlled Release* 2017; 262: 58-71.
40. Nikyar A, Bolhassani A, Rouhollah F, Heshmati M. In vitro delivery of HIV-1 Nef-Vpr DNA construct using the human antimicrobial peptide LL-37. *Curr Drug Delivery* 2022; 19: 1083-1092.
41. Jinek M, Chylinski K, Fonfara I, Hauer M, Doudna JA, Charpentier E. A programmable dual-RNA-guided DNA endonuclease in adaptive bacterial immunity. *Science* 2012; 337: 816-821.

Khairkhah et al.

42. Rasul MF, Hussien BM, Salihi A, Ismael BS, Jalal PJ, Zanichelli A, Jamali E, Baniahmad A, Ghafouri-Fard S, Basiri A. Strategies to overcome the main challenges of the use of CRISPR/Cas9 as a replacement for cancer therapy. *Mol. Cancer* 2022; 21: 64.
43. Moreno-Angarita A, Aragón CC, Tobón GJ. Cathelicidin LL-37: A new important molecule in the pathophysiology of systemic lupus erythematosus. *Journal of Translational Autoimmunity* 2020; 3: 100029.
44. Zhang X, Oglęcka K, Sandgren S, Belting M, Esbjörner EK, Nordén B, Gräslund A. Dual functions of the human antimicrobial peptide LL-37-target membrane perturbation and host cell cargo delivery. *Biochimica et Biophysica Acta (BBA)-Biomembranes* 2010; 1798: 2201-2208.
45. Chamilos G, Gregorio J, Meller S, Lande R, Kontoyiannis DP, Modlin R, Gilliet M. Cytosolic sensing of extracellular self-DNA transported into monocytes by the antimicrobial peptide LL37. *Blood, The Journal of the American Society of Hematology* 2012; 120: 3699-3707.
46. Yoshihara T, Saga Y, Urabe M, Uchibori R, Matsubara S, Fujiwara H, Mizukami H. CRISPR/Cas9-mediated cervical cancer treatment targeting human papillomavirus E6. *Oncol. Lett.* 2019; 17: 2197-2206.
47. Inturi R, Jemth P. CRISPR/Cas9-based inactivation of human papillomavirus oncogenes E6 or E7 induces senescence in cervical cancer cells. *Virology* 2021; 562: 92-102.
48. Noroozi Z, Shamsara M, Valipour E, Esfandiyari S, Ehghaghi A, Monfaredan A, Azizi Z, Motevaseli E, Modarressi MH. Antiproliferative effects of AAV-delivered CRISPR/Cas9-based degradation of the HPV18-E6 gene in HeLa cells. *Sci. Rep.* 2022; 12: 2224.
49. Ehrke-Schulz E, Heinemann S, Schulte L, Schiwon M, Ehrhardt A. Adenoviral vectors armed with papillomavirus oncogene specific CRISPR/Cas9 kill human-papillomavirus-induced cervical cancer cells. *Cancers* 2020; 12: 1934.
50. Taha EA, Lee J, Hotta A. Delivery of CRISPR-Cas tools for in vivo genome editing therapy: Trends and challenges. *J. Controlled Release* 2022; 342: 345-361.
51. Ye J, Liu E, Yu Z, Pei X, Chen S, Zhang P, Shin MC, Gong J, He H, Yang VC. CPP-assisted intracellular drug delivery, what is next? *International Journal of Molecular Sciences* 2016; 17: 1892.
52. Henzler-Wildman KA, Martinez GV, Brown MF, Ramamoorthy A. Perturbation of the hydrophobic core of lipid bilayers by the human antimicrobial peptide LL-37. *Biochemistry* 2004; 43: 8459-8469.
53. Wu WK, Wang G, Coffelt SB, Betancourt AM, Lee CW, Fan D, Wu K, Yu J, Sung JJ, Cho CH. Emerging roles of the host defense peptide LL-37 in human cancer and its potential therapeutic applications. *International Journal of Cancer* 2010; 127: 1741-1747.
54. Kuroda K, Okumura K, Isogai H, Isogai E. The human cathelicidin antimicrobial peptide LL-37 and mimics are potential anticancer drugs. *Frontiers in Oncology* 2015; 5: 144.
55. Coffelt SB, Waterman RS, Florez L, Bentrup KHZ, Zwezdaryk KJ, Tomchuck SL, LaMarca HL, Danka ES, Morris CA, Scandurro AB. Ovarian cancers overexpress the antimicrobial protein hCAP-18 and its derivative LL-37 increases ovarian cancer cell proliferation and invasion. *International Journal of Cancer* 2008; 122: 1030-1039.
56. Weber G, Chamorro CI, Granath F, Liljegren A, Zreika S, Saidak Z, Sandstedt B, Rotstein S, Mentaverri R, Sánchez F. Human antimicrobial protein hCAP18/LL-37 promotes a metastatic phenotype in breast cancer. *Breast Cancer Res.* 2009; 11: 1-13.
57. Zhou X, Jiang W, Liu Z, Liu S, Liang X. Virus infection and death receptor-mediated apoptosis. *Viruses* 2017; 9: 316.
58. Jiang P, Yue Y. Human papillomavirus oncoproteins and apoptosis. *Experimental and Therapeutic Medicine* 2014; 7: 3-7.
59. Arjomandnejad M, Muhammadnejad A, Haddadi M, Sherkat KN, Rismanchi S, Amanpour S, Muhammadnejad S. HeLa cell line xenograft tumor as a suitable cervical cancer model: growth kinetic characterization and immunohistochemistry array. *Arch. Iran Med.* 2014; 17(4): 273-277.
60. Galus R, Wlodarski P, Wlodarski K. Fluvastatin increases heterotopically induced ossicles in mice. *Clin. Exp. Pharmacol. Physiol.* 2006; 33: 388-390.

Cite this article:

Khairkhah N, Bolhassani A, Najafipour R, Namvar A, Milani A, Agi E, Anvar A, Khosravy MS. Inhibition of HPV18 E6/E7 Protein-Expressing HeLa Cell Proliferation Using Optimized De Novo CRISPR/Cas9 Constructs Delivered by the LL-37 Peptide. *J Med Microbiol Infect Dis*, 2024; 12 (4): 278-291. DOI: 10.61186/JoMMID.12.4.278.